Declaration of Interest Statement

Declaration of interests

☒The authors declare that they have no known competing financial interests or personal relationships that could have appeared to influence the work reported in this paper.

☐The authors declare the following financial interests/personal relationships which may be considered as potential competing interests:

Title Page with Author Information

Smart Quick Response code for multianalyte determination

Antonio Marín-Sánchez [a], Inmaculada Ortiz-Gómez [a, c], David Gallego-Méndez [a, c], Carlos Rodríguez-Domínguez [d], Luís Fermín Capitán-Vallvey [a, c], Diego P Morales [b, c], José Antonio Álvarez-Bermejo [e, *], Encarnación Castillo [b, c], Alfonso Salinas-Castillo [a, c,*]

[a]ECsens, Department of Analytical Chemistry, Faculty of Sciences, 18071 University of Granada, Granada, Spain.

[b]Research Group, Department of Electronics and Computer Technology, Faculty of Sciences, 18071 University of Granada, Spain

[c]Unit of Excellence in Chemistry applied to Biomedicine and the Environment, University of Granada, Spain

[d]Department of Software Engineering, Faculty of Education, Economy and Technology of Ceuta, University of Granada, Spain

[e]Department of Information Technology, University of Almeria, Cañada de San Urbano, 04120, Almería, Spain

[*]Corresponding author: E-mail address: alfonsos@ugr.es (Alfonso Salinas-Castillo) and jaberme@ual.es (José Antonio Álvarez-Bermejo)

Smart Quick Response code for multianalyte determination

Abstract

The extensive use of smartphones with point-of-care applications has bolstered the development of what has come to be known as Healthcare 4.0. The ability to track biomarker parameters has become an essential part of monitoring the evolution of certain diseases, with the potential for application with a large selection of population groups. In that vein, this work presents a multianalyte quick response (QR) colorimetric code for the real-time measurement of glucose and lactate samples using smartphones. The colorimetric QR code contains both the QR static data and the dynamic information from the sample analyses. Two correction methods are applied in order to compensate for the variation in the surrounding conditions in the determination of the biomarkers. Glucose and lactate recovery between 91 and 117% was found for assays with sweat and serum samples using a smartphone readout. The developed system demonstrates flexible measurement conditions for using in real situations.

Keywords

Colorimetric · Glucose · Lactate · QR code · paper-based · smartphone

1. Introduction

Currently, one of the main issues facing society is guaranteeing quality access to healthcare systems [1]. In that respect, the Internet of Things (IoT), cloud computing and many other emerging computing paradigms are being applied to enhance and promote what has come to be known as Healthcare 4.0 [2]. One of the key advantages of Healthcare 4.0 is that it allows people to continuously track their biometric data and notify healthcare professionals when they show signs of pathology. Additionally, the evolution of many chronic diseases, such as diabetes and hypertension, can be continually monitored, thus preventing some of the most dangerous consequences associated with them.

Additionally, point-of-care (POC) frameworks and platforms improve the degree of interconnection between patients and experts, between data sources and data sinks. More specifically, smartphone based POC developments and deployments have been thoroughly

studied in the literature due to the widespread dissemination of smartphones in society and the low-cost solutions that can provide [3], [1], [4], [5]. Colorimetric tests, in particular, are one of the most researched techniques due to their inherent subjectivity and high human perception dependency [6], [7], [8], [9], [10], [11], [12], [13], [14], [15], [16], [17].

However, these solutions do not increase sample traceability, that is, the sample cannot be tracked throughout interconnected and diverse healthcare systems. One feasible solution is to extend quick response (QR) codes [18] to use as microfluidic paper-based analytical devices (μPAD,) depositing or immobilizing the reagents in some regions of the QR code, which will undergo a colour change in the presence of the analyte sought. While QR codes usually only store static data (e.g., patient ID, sample ID, etc.), here the analyte in the sample generates a colorimetric signal that can be automatically processed by a smartphone and therefore be connected to, for example, a patient's clinical record. Combining the QR code information with the data provided by the colorimetric signals that can dynamically appear is possible due to the error correction capability of QR codes. The combination of QR codes with dynamic colorimetric data makes possible to standardize the sensor detection procedure and avoids having to design complex geometrical image processing algorithms. Although similar research has been conducted in [19], [20], [21], [22], [23], [24], [25] this paper operates with different devices and brightness conditions.

Although QR code paper-based analytical devices that use smartphones as a measurement system are truly cost-effective POC solutions, some issues remain to be resolved to obtain a practical solution. One of the most restricting issues related to pairing POC and smartphones is the fact that the sensor needs to be properly oriented to read the dynamic information in the correct position when it appears. However, the orientation and positioning of the smartphone during the measurement cannot be limited, as this would negatively impact the user's experience and could affect the sensor data gathering procedure. Additionally, the QR code detection application must operate on different mobile devices, but the built-in camera parameters cannot be fixed, because every smartphone manufacture provides their own algorithms to process, handle and enhance the image as it is captured by the camera. Moreover, even two devices from the same manufacturer and same model can have different cameras, as the manufacturing process prints differences in the camera sensors. The most

concerning issue that remains to be addressed is the fact that the system needs to make correct measurements under different light conditions. When not addressed properly, all of these issues lead to non-robust solutions.

Providing a QR paper-based analytical measurement system that is enhanced (by exploiting the code theory behind it) to resolve the abovementioned concerns would increase the performance, reliability and accuracy of the individual measurements. As the proposed solution relies on the use of smartphone devices that are able to add metainformation (i.e., enriching it) to the data gathered from the measured sample by adding the static data from the QR – or data extracted from any sensor installed in the device to detect, for example, location, temperature, atmospheric, pressure, etc. – and can also connect to Internet services, a cloud computing service has been designed to collect and build intelligence using the measurements and samples under study. Cloud computing is a technological paradigm in which computing resources are offered on-demand through an Internet connection by a set of remote services [26]. The main idea behind this paradigm is to enable the end-user's software to access as many resources as required to accomplish their goals, regardless of the local computing resources in the user's device. The cloud computing platform makes it possible to track samples, contrast different samples, correct measurements and the like.

This work introduces an enzymatic QR code sensor integrated solution designed to measure glucose and lactate levels in sweat and serum samples. The paper provides an explanation of the design and development process of the enzymatic QR code, its architecture and the design of the smartphone application, and explains the results and performance of the solution during the experiments conducted with real samples of sweat and serum. To test the accuracy of the measurements, both estimated and real analyte concentrations are used. The response of the enzymatic QR code to different devices, the smartphone positioning and light conditions are also analysed. In addition, the cloud computing platform developed to complement the measurement system is described. This work proposes the cloud computing platform as a shared repository of samples and their measurements combined with metainformation to further expand the information processing or simply track the samples.

2. Experimental

2.1. Reagents and materials

Glucose, fructose, urea, uric acid, lactate, pyruvic acid, sodium chloride (NaCl), potassium chloride (KCl), ammonium chloride (NH_4Cl), magnesium chloride ($MgCl_2$), calcium chloride ($CaCl_2$), calcium sulfate ($CaSO_4$), sodium hydrogen carbonate ($NaHCO_3$), sodium dihydrogen phosphate (NaH_2PO_4), DL-cysteine (Cys), horseradish peroxidase (HRP), glucose oxidase (GOx), lactate oxidase (LOx), 3,3',5,5'-tetramethylbenzidine (TMB) and ethanol were purchased from Sigma Aldrich. All reagents were of analytical reagent grade unless stated otherwise. Whatman No 1 chromatography paper from Sigma-Aldrich is used to print the QR code. All aqueous solutions were made using reverse-osmosis type quality water (Milli-RO 12 plus Milli-Q station from Millipore, conductivity 18.2M Ω•cm).

2.2. Hardware and software

The images described by the QR code are acquired with three different devices. A digital camera, Sony Cyber-shot DSC-HX 300 (Sony, Tokyo, Japan) is employed for calibration process. To keep all the image-gathering conditions the same, a Cube Light Box [27] is used with the camera placed in front of a homemade white wooden box with two LED 6500 K lamps placed at 45° with respect to the digital camera, with the μPAD in a fixed position inside the box to isolate it from external radiation. The smartphones used to decode the QR codes and the information hosted in them are: Pocophone F1 (Xiaomi Corporation, Hidian, China) and Huawei PSmart (Huawei Technologies Co. Ltd., Shenzhen). The Pocophone F1 has a 12 + 5 megapixel, dual pixel autofocus built-in camera with a CCD sensor; 6 GB RAM and a Snapdragon 845 processor (Xaomi, 2020). The Huawei PSmart has a 13 + 2 megapixel, dual pixel autofocus built-in camera with a CCD sensor; 3 GB RAM and a Kirin 659 processor (Huawei, 2020). A Xerox ColorQube 8580 digital wax printer (Xerox Corporation, Norwalk, CT, USA) is used to print the QR code and a 3D printer from Formlabs (Formlabs, Form 3, USA) is used to make a plastic device to handle the sensing QR code.

Additional software suites are used, as follows: (1) MATLAB: all the algorithms implemented in the smartphone devices are previously validated by running simulations and proof of concepts; (2) Android Studio: the development suite used to code the Android application for the colorimetric QR code analysis. This analysis is handled by a ZXing library, a popular open source library for QR code related processing [28] and the library is

redesigned to extract the RGB values from the colorimetric QR code; (3) Adobe Illustrator: used to design the colorimetric QR codes.

2.3. Calibration colour reference

A reference curve printed in the QR code is used to correct the colour of the samples. This curve consists of five blue points, which represent a linear variation of saturation from 10% to 90%, printed in the QR code as shown in Figure S1. The aim of the calibration process is to map each point on the reference curve with a concentration value for each analyte. This obtains the analytical curves of the analytes (in this case, glucose and lactate), which also present a variation in saturation. In the calibration process, both curves (the printed reference and analytical curves) are acquired under standard measurement conditions using the Sony DSC-HX300 camera in the Cube Light Box. The camera is set up as follows: 1920 x 1080 pixel resolution, f/2.2 aperture value, 1/50 s exposure time, ISO-160, 2800 K white balance, with the images saved in a jpg format.

As a result of this process, a standardized reference curve and two standardized analytical curves (one for each analyte) are pre-loaded in the software for use by the colour correction algorithms every time that a QR code is analysed by the smartphone.

2.4. Fabrication and preparation of the QR code for biosensor analysis

A Xerox ColorQube 8580 wax printer is used to print the designed QR code on Whatman No 1 chromatography paper. This design includes three layers, as shown in Figure 1: the typical black QR areas with static information, the printed modules of the reference curve, and the biosensor modules. Then, using a micropipette, 0.2 µL TMB (20 mM) and 0.2 µL of HRP (156 U/mg) and 0.2 µL of GOx (160 U/mL) prepared in 1 mg/mL chitosan in phosphate buffered saline (PBS; pH 7.4, 10 mM) are added to the biosensor modules of the QR code for glucose detection. The modules for lactate detection are also prepared according this procedure, but using LOx (150 U/mL) instead of GOx. After each addition, the QR code is dried for 5 minutes.

A plastic device to handle the sensing paper during the experiments is designed and created on a 3D printer, see Figure 1. This 3D handling device is composed of three parts: (1) the printed QR code on paper that contains the reagents for the determination of glucose and

lactate in the selected modules, (2) an absorbent pad for sampling, and (3) a transparent screen to assemble the absorbent pad and the QR code.

Figure 1

2.5. Measurement procedure and extraction of the coloured signal

In a typical process for simultaneous glucose and lactate determination, the handling device (Figure 1) is immersed in solutions containing glucose and/or lactate. The sample is collected by the absorbent pad and moves towards the QR code by capillary action, where the colorimetric analysis is conducted. Once the sample reaches the QR code, it is kept at room temperature for 15 min to complete the colorimetric reaction. Once this reaction is completed, a blue colour appears in the measurement modules for glucose and lactate. To optimize the colorimetric assay conditions, the QR code is placed in a Cube Light Box in a fixed position and then digitalized using one of the smartphones described in Subsection 2.2.

To extract the colorimetric signal from the QR code using a smartphone, an Android based ZXing library is used. This library was modified in order to perform the acquisition of the static data and colorimetric signals by extracting the RGB matrix from the QR code, which is usually generated in a YUV format (a typical luminance and chrominance-based image format). The steps of the algorithm to extract the colorimetric signals from the modules are:

- Detect the QR code using a local threshold over the luminance channel [28].
- Obtain the RGB values of each module from the colorimetric QR (the ZXing library is modified to support this step).
- Create the RGB QR code matrix from the RGB image (the ZXing library is modified to support this step).
- Acquire the RGB signals for the reference and analyte modules. The positions of these modules need to be set in the system to allow the system to identify the modules from which the RGB signals are extracted.

As a result of the data acquisition process, both RGB signals are obtained: the RGB signal measured from the analyte modules, rgbm, and the RGB signal extracted from the reference

modules, rgbr. Then, the RGB signal can be converted to another colour space, such as HSV, depending on the channel in which the reference curve is measured, see Subsection 3.4.

2.6. Glucose and lactate biosensing using standard

To investigate the correlation between glucose and lactate concentration and registered color change, paper circles of 10 mm diameter were printed on cellulose filter paper by a wax printer, and the wax barriers were generated by heating the paper at 125˚C for 5 min in an oven. Next, a 5 µL TMB (20 Mm), 5 µL of HRP (156 U/mg) and 5 µL of GOx (160 U/mL) or LOx (150 U/mL) prepared in 1 mg/mL chitosan in phosphate buffered saline (PBS; pH 7.4, 10 mM) were dropped onto the paper circles. The colorimetric assay was carried out using glucose and lactate standard solutions with predetermined concentration levels (150-4000 µM) and allowed to react on paper for 15 minutes.

The S coordinate of the HSV colour space was used such as the analytical parameter because we could be observed that the saturation was directly proportional to the concentration of both analytes (glucose and lactate) spiked samples, Figure S2. To quantitatively analyse the results of the assay, we took a photo of the paper circle after reaction with glucose or lactate standards using a smartphone and digitized the colour change of the obtained images using the ImageJ software. The saturation of HSV colour space increased with the increase in glucose and lactate concentration. The colour change could be clearly distinguished at 15 minutes.

2.7. Analysis of biological samples

To investigate the suitability and efficiency of the application in real environments, the simultaneous determination of glucose and lactate in two complex biological fluids (serum and artificial sweat) is performed. Human serum obtained from anonymous healthy volunteers were analysed. On the other hand, the artificial sweat samples are prepared according to the following composition: 0.08 g/L $MgCl_2$, 4.67 g/L NaCl, 0.45 g/L KCl, 0.27 g/L NH_4Cl, 0.13 g/L $CaSO_4$, 0.22 g/L $NaHCO_3$, 0.005 g/L NaH_2PO_4, 0.60 g/L urea, 0.004 g/L uric acid, 0.07g/L pyruvic acid and 0.002 g/L ascorbic acid. After preparation, the pH is adjusted to 6.5 [29]. The samples are spiked with a fixed glucose and lactate standard solution. After that, the samples are filtered through a 0.22 µm filter and are diluted one hundred times with purified water. Finally, the detection of both analytes is done following

the measurement procedure, and the contents of the glucose and lactate in the samples are calculated according to an analytical function acquired from the standard solutions.

3. Results and discussion

3.1. Overview scheme of the system

To explain the internals of the system and how it operates, its elements are briefly presented based on the general scheme of the system as depicted in Figure 2. As described in Subsection 2.4, the QR code is designed by overlapping three layers: the supporting layer for the QR code encoded data (static information), the reference modules, and the biosensor modules for analytical detection (dynamic information). The QR code is integrated into the handling device, making it easy-to-use and handy and preventing damage to the code and biosensor. This also facilitates analysis from any angle, a desirable feature when operating CCD cameras integrated into smartphone devices. The QR code analyser software, as implemented in the smartphone, is able to decode the QR data (static) and the sample information (dynamic) that it contains. The data obtained is not affected by different issues (e.g. light, the smartphones acquiring the image). Rather, all these potential errors are compensated for by the code correction algorithm inherent to the QR codes. After the decoding stage, the software runs algorithms to extract and correct the colour of the analyte and determine the concentration using the analytical curves from the calibration. The colour correcting algorithms employ two different methods: white and black (W/B) and reference colour curve corrections (R/C). In this article, serum and sweat samples are determined by the application. Once the data is decoded and the concentration obtained, all the information processed by the smartphone is sent to the cloud computing facility designed to share and interconnect the analysis data with any other online service that might need it for further processing tasks.

Figure S1 presents the design of the colorimetric QR code. The blue modules are the printed colour reference modules and the three green corner squares are used for the W/B method. The reference colour modules are designed in such a way as to generate linear variation in saturation, as seen in Figure S1. This curve relates the saturation measured, Sm, through a linear equation, with the saturation theoretically printed, Sp. The reference modules are distributed along the QR code in order to better obtain the brightness variations. The biosensor modules, those marked with molecule symbols, can be placed anywhere on the remainder of the QR code, assuming that the brightness is spatially invariant. The saturation

of the biosensor module is associated with a saturation value of the printed colours by the reference curve. In non-standardized conditions, these reference curves shift from the standardized curve, and the correction methods are applied to correct the colour of the analyte. The system makes it possible to measure a set of analytes with similar colorimetric TMB system changes using the same reference curve to correct them.

Figure 2

3.3. W/B correction

Figure 3 presents the architecture of the system and the stages followed by the colorimetric signal. The RGB signals obtained from the smartphone are corrected using the W/B method and converted to a specific colour space. In this case, the saturation channel of the HSV colour space shows a linear variation with the concentration of glucose and lactate. Therefore, saturation is the predefined magnitude of the colorimetric signals and, consequently, the reference curve is designed to be linear in saturation. The W/B method is a typical brightness correction process that has been applied earlier in the literature [7], [21]. This method uses white and black to correct the RGB signals and obtain new RGB corrected values, as in Equation 1

$$\boldsymbol{rgb_c} = \frac{255}{(\boldsymbol{rgb_w} - \boldsymbol{rgb_b})}(\boldsymbol{rgb_m} - \boldsymbol{rgb_b}) \quad (1)$$

where rgb_c and rgb_m are the corrected and measured RGB values, and rgb_b and rgb_w are the RGB values of the black and white squares in the green regions in Figure S1. Then, the saturation of the RGB corrected signal is extracted, providing both analyte and reference saturation signals (see Figure 3). In this case, the correction is quite important. Low saturation values of the reference curve are highly influenced by the colour temperature of the light source, deforming the curve tendency, and the W/B method corrects this error perfectly. To apply this method, the brightness has to be the same throughout the entire region of the QR code, which is a reasonable supposition for QR code sizes used here, 22 mm. Additionally, there can be no shadowed areas in the code, in order to comply with this supposition.

Figure 3

3.4. R/C correction

At this point, all the signals mentioned have been W/B corrected (see Figure 3). The next stage is the application of the reference curve, R/C, a method to correct the deviation between the measured reference colour modules, r_m, and standardized reference signal, r_s. These curves relate the measured saturation, S_m, with the saturation theoretically printed, S_p. Both curves are derived from the same printed reference modules in the QR code, but measured at different conditions. The r_s signal is measured in the controlled experimental conditions and pre-loaded in the software, as discussed in Subsection 2.3. However, r_m is measured in real conditions. As shown in Figure S1 in Subsection 3.2., the reference signals can be seen as reference curves modelled with a linear equation, where am, b_m and a_s, b_s are the linear coefficients of r_m and r_s. The typical deviation of both curves is presented as a rotation between them, with an angle α, as seen in Figure S3. This curve shift is further discussed below in Section 3.7. The R/C method calculates this rotation using Equation 2, and the rotation is then applied to the measured analyte to obtain a standardized measurement (m_2, p_2) using Equations 3 and 4. In Equations 3 and 4, the point (m_1, p_1) is the value of the measured analyte in the r_m curve, and (m_0, p_0) is the cut point between r_m and r_s. With this method, m_2 is the standardized saturation, and the concentration of the analyte can be calculated using the analytical calibration curves entered into the smartphone beforehand, see Subsection 2.3.

$$\alpha = \tan^{-1}\left(\frac{b_m - b_s}{1 + a_m a_s}\right) \quad (2)$$

$$p_2 = (p_1 + p_o)\cos(-\alpha) - (m_1 - m_o)\sin(-\alpha) + p_o \quad (3)$$

$$m_2 = (p_1 - p_o)\sin(-\alpha) + (m_1 - m_o)\cos(-\alpha) + p_o \quad (4)$$

3.5. Analytical characterization of the colorimetric QR code

The analytical curves for glucose and lactate are obtained in the ambient conditions described in Subsection 2.3. The blue colour of the biosensor modules of the colorimetric QR code is followed by the S saturation coordinates of the HSV colour space after imaging with a camera. The S value increases with the glucose and lactate concentration in each case. The analytical function is obtained by means of a calibration set composed of 5 glucose and lactate standards. The concentration rankings for glucose and lactate are from 200 to 1000 µM, using 15 minutes as the reaction time. The resulting calibration curve for glucose and lactate is presented in Figure S4. The dependence between the S value and glucose or lactate concentration obtained with a smartphone presented a correlation coefficient of R^2= 0.9529

for glucose and R^2=0.9051 for lactate, indicating a wide linear response for both compounds in each case. Using a linear fitting, the regression equation for glucose and lactate are y = 0.05x + 15.63 and y = 0.05x + 11.37, respectively. The detection limit (LOD) is defined by the equation LOD = (3σ/s) at the signal-to-noise of 3, where σ is the standard deviation of the blank signals and s is the slope of the calibration curve. Based on this equation, the LOD for glucose is calculated to be 65.21 μM and 43.16 μM for lactate. The reproducibility of the proposed sensing system for glucose and lactate was also studied. The relative standard deviation (RSD) is 1.20% and 0.80% for each compound at 200 μM for 6 repeated measurements, respectively. A summary of the analytic characteristics is shown in Table 1.

A comparative study of different procedures for the colorimetric detection of glucose and lactate using paper devices from the literature is presented in Table S1. Compared to existing colorimetric methods for glucose and lactate detection, the developed colorimetric QR code offers a good sensitivity and detection limit. These analytical curves are applied in the last stage of the system architecture, see Figure 3. Thus, once the biosensor modules (analytes) are W/B corrected and R/C corrected, this saturation value is entered in one of the two analytical curves (glucose or lactate) and the real concentration is obtained.

Table 1

3.6. Study of reference curve variations for different smartphone and illumination conditions

Figure S5a presents an average of 24 reference curves measured from colorimetric QR codes with the two different smartphones described in Subsection 2.2. The QR code size is 22 mm and the measurement distance is 8 cm. For these experiments, the camera parameters are automatically controlled by the smartphones, and a LED lamp (3000 K) is used as the light source. The behaviour of the reference curve is linear with both devices. An increase in the slope of the curve is found with Huawei PSmart. The standard deviation of saturation for both devices is quite similar, 5.6 for Pocophone F1 and 6.6 for Huawei PSmart. Therefore, there are no significant differences between the data obtained for the two devices. Figures S5b and S5c present a study of the reference curve shift after W/B correction under different illumination conditions performed using the Huawei PSmart. As Figure S5a shows, when the ISO changes, the W/B correction is able to considerably correct the variations of the curve.

However, if the white balance is varied by changing the colour temperature, the W/B correction cannot correct these deviations correctly, as Figure S5c shows.

Figure 4 shows the saturation of the measured modules for a colorimetric QR code at different colour temperatures, before and after both correction methods (W/B and R/C). A decrease in the saturation is noted as the colour temperature increases, as Figure 4a shows. However, this tendency is completely corrected after the RC correction method, as shown in Figure 4a. As a result, the error increases slightly after this process. A similar study of the saturation variation of the measured modules for the same colorimetric QR code is performed for different ISOs in Figure 4b. In this case, there are no significant variations between different ISO conditions. However, when the R/C correction is applied, the saturation tends to increase up to 80%, which is the expected value of these measured modules. Consequently, the double correction method applied is able to correct the complex deviation of the curve and reliably measure the saturation of the modules under different illumination conditions.

Figure 4

3.7. Study of the measurement angle and QR size

The optimization of the measurement conditions is performed using the Huawei PSmart. The reference curve of a QR colorimetric code is analysed for different measurement distances, QR code sizes, and measurement angle. Additionally, the module area, which is the size in pixel of each module of the QR code, is analysed. Figure S6a presents a study of the relation between the module area and the measurement distance for several QR code sizes. As can be observed, a decrease in the module area is seen as the distance increases. The minimum measurement distance is seen when the QR code occupies the entire measurement rectangle on the smartphone screen. The minimum distance is normally the best distance to measure the QR code but, when the measurement distance is less than the focal distance of the smartphone, the module area decreases dramatically. This occurs when the QR size is below approximately 13 mm. In addition, for this QR code size, the QR code cannot be detected for distances beyond 6 cm.

Figure S6b shows the reference curve for the different measurement distances with a QR size of 22 mm. A decrease in the slope of the reference curve is seen as the measurement distance

increases. Figure S6c presents the reference curve for different module areas. A similar behaviour in the reference curve is noted for module areas above 17 pixels, although the slope of the reference curve significantly decreases below this value. Figure S6d presents the reference curve for three different measurement angles at the minimum distance. No variations in the reference curve are noted as the angle changes, but when the angle is larger than 40º, the QR code is not detected at the minimum distance. Thus, the optimal measurement conditions of the system are the minimum measurement distance with a QR code large enough to be focused correctly and with an angle between 0 and 40°.

3.8. Selectivity

The biological samples contain different species such as uric acid, NaCl, $CaCl_2$, $MgCl_2$, fructose, cysteine, glucose and lactate could induce interference in the glucose and lactate determination. The interference study evaluates the effects of these species on the detection of glucose and lactate. Figure S7 shows the selectivity results measured and processed with a Huawei device. The sample solutions containing the interferences are measured using fourteen different QR codes. The concentrations of the seven tested interferences are 800 µM. In comparison, samples containing only the interference show low saturation values. Thus, the QR codes exhibit high selectivity and can be applied for the multiplexed detection of glucose and lactate in mixtures. The good selectivity is mainly due to the high specificity of the enzymatic colorimetric reactions.

3.9. Stability study

The storage stability of the developed QR code to detect glucose and lactate was investigated over the course of thirteen consecutive days. The QR codes are stored in dark, dry sealed conditions at 4°C and tested every week. No significant change in the colorimetric responses are observed for both analytes for at least 30 days, as shown in Figure S8. Thus, the storage stability of the QR code is acceptable and is available for clinical diagnostics and point-of-care testing.

3.10 Biological sample application

For the simultaneous detection of glucose and lactate in serum and sweat samples, these samples are spiked with 200, 500 and 800 µM glucose or lactate standard solutions. The experiments are run in triplicate for each concentration of glucose and lactate. The results are shown in Table 2 and Table 3 for the Huawei PSmart and Pocophone F1 devices,

respectively. The recoveries obtained are in the range of 100-117% for glucose and 91-108% for lactate. There are no differences between the results obtained for both smartphones. As a result, our system is able to work on different devices.

Table 2

Table 3

3.11. End-user software applications

A smartphone application has been developed that integrates a QR code and a data viewer. This smartphone application is easy to use, and does not require any previous training to capture the samples. It automatically updates, from time to time, to the latest scan configuration parameters. In this way, we ensure that, as a error correction code is improved or new QR code formats integrated (e.g., for the analysis of newer samples), the end users will always have up-to-date and optimal scan capabilities.

Figure S9 shows screenshots of the smartphone application work-flow. Figure S9a presents a register of the analysis performed where a user can add a new analysis or obtain the information about each one. The user has two options to add a new QR register from an image in the gallery or by taking a picture in-situ (Figure S9b). Figure S9c shows an example of a preview of the analysis where the user can name the register and check that the image is adequate. After the QR code is detected, the application runs the data viewer to provide a preview of the colorimetric QR code and the concentration measured for glucose and lactate samples, as shown in Figure S9d.

3.12. Cloud system architecture

Cloud computing is used in our proposal to provide a set of backend services mainly to track and share measurements from samples, creating a repository. Figure 5 depicts the different hardware and software components developed in this study. These components are categorized into three main layers: application, platform and infrastructure. The application layer contains end-user components: a mobile application, a management Web application, QR codes and a custom-designed QR code analyser.

The platform layer contains a set of high-level services that are directly used by the components of the application layer. A notification service makes it possible to send messages to end users whenever an important event happens in the overall system (availability of new tests, important news, etc.). A chemical information system stores structured, multimedia data regarding the different chemical tests that the system offers. Moreover, the identification and authorization service provides editing access to the chemical information system.

The infrastructure layer is composed of a set of low-level services to store structured information and files or to access the internal services offered by the Cloud computing provider. Finally, a set of security policies are imposed across the different layers: data and Internet connection encryption, automatized backups, user privacy, etc. Table S2 includes a description of the components of each layer.

Figure 5

4. Conclusions

The system proposed in this work presents a fully integrated smartphone POC solution to perform colorimetric analyses of biological samples embedded in a QR code. The system developed is totally functional with regard to extracting the concentration of the analytes through an image of the sample and its calibration curve, without any additional processing. This system is able to perform analyses of several substances simultaneously in one shot, using a low-cost device and smartphone. The integration of the samples in a QR code reduces the traceability of the samples and also makes it possible to connect a cloud system to the instantly obtained results. Moreover, the brightness correction method developed in this study is able to correct complex changes in luminosity conditions, such as variations in the white balance and ISO in order to obtain a calibrated measurement. The system comes with access to a custom cloud platform with a four-layer architecture (infrastructure, platform, application and security) to enable several functionalities, such as notifications and user-identification and to manage a chemical information system. Moreover, future interconnections are possible between the findings of this study work and external healthcare information systems, providing reliability, scalability and security to the system. In short, the

system developed is a promising POC solution (device, algorithms and cloud architecture) with high scalability and reliability for implementation in health care.

Acknowledgements

This work was funded by the Spanish Ministerio de Economía y Competitividad (Projects PID2019-103938RB-I00, PID2020-117344RBI00 and CTQ2017-86125-P) and the Junta de Andalucía (Projects B-FQM-243-UGR18, P20_00265 and P18-RT-2961). The projects were partially supported by European Regional Development Funds (ERDF).

Conflicts of interest

There are no conflicts to declare.

References

[1] I. Hernández-Neuta *et al.*, "Smartphone-based clinical diagnostics: towards democratization of evidence-based health care," *J. Intern. Med.*, vol. 285, no. 1, pp. 19–39, Jan. 2019, doi: 10.1111/joim.12820.

[2] P. P. Jayaraman, A. R. M. Forkan, A. Morshed, P. D. Haghighi, and Y. Kang, "Healthcare 4.0: A review of frontiers in digital health," *WIREs Data Min. Knowl. Discov.*, vol. 10, no. 2, Mar. 2020, doi: 10.1002/widm.1350.

[3] D. Quesada-González and A. Merkoçi, "Mobile phone-based biosensing: An emerging 'diagnostic and communication' technology.," *Biosens. Bioelectron.*, vol. 92, pp. 549–562, Jun. 2017, doi: 10.1016/j.bios.2016.10.062.

[4] K. Yang, H. Peretz-Soroka, Y. Liu, and F. Lin, "Novel developments in mobile sensing based on the integration of microfluidic devices and smartphones," *Lab Chip*, vol. 16, no. 6, pp. 943–958, Mar. 2016, doi: 10.1039/C5LC01524C.

[5] S. Kanchi, M. I. Sabela, P. S. Mdluli, Inamuddin, and K. Bisetty, "Smartphone based bioanalytical and diagnosis applications: A review," *Biosens. Bioelectron.*, vol. 102, pp. 136–149, Apr. 2018, doi: 10.1016/j.bios.2017.11.021.

[6] L. Shen, J. A. Hagen, and I. Papautsky, "Point-of-care colorimetric detection with a

smartphone," *Lab Chip*, vol. 12, no. 21, p. 4240, 2012, doi: 10.1039/c2lc40741h.

[7] J. Il Hong and B.-Y. Chang, "Development of the smartphone-based colorimetry for multi-analyte sensing arrays," *Lab Chip*, vol. 14, no. 10, pp. 1725–1732, 2014, doi: 10.1039/c3lc51451j.

[8] A. K. Yetisen, J. L. Martinez-Hurtado, A. Garcia-Melendrez, F. da Cruz Vasconcellos, and C. R. Lowe, "A smartphone algorithm with inter-phone repeatability for the analysis of colorimetric tests," *Sensors Actuators B Chem.*, vol. 196, pp. 156–160, Jun. 2014, doi: 10.1016/j.snb.2014.01.077.

[9] M.-Y. Jia, Q.-S. Wu, H. Li, Y. Zhang, Y.-F. Guan, and L. Feng, "The calibration of cellphone camera-based colorimetric sensor array and its application in the determination of glucose in urine," *Biosens. Bioelectron.*, vol. 74, pp. 1029–1037, 2015, doi: 10.1016/j.bios.2015.07.072.

[10] A. Y. Mutlu, V. Kılıç, G. K. Özdemir, A. Bayram, N. Horzum, and M. E. Solmaz, "Smartphone-based colorimetric detection via machine learning," *Analyst*, vol. 142, no. 13, pp. 2434–2441, Jun. 2017, doi: 10.1039/C7AN00741H.

[11] X. Bao, S. Jiang, Y. Wang, M. Yu, and J. Han, "A remote computing based point-of-care colorimetric detection system with a smartphone under complex ambient light conditions," *Analyst*, vol. 143, no. 6, pp. 1387–1395, 2018, doi: 10.1039/C7AN01685A.

[12] M. Ra, M. S. Muhammad, C. Lim, S. Han, C. Jung, and W.-Y. Kim, "Smartphone-Based Point-of-Care Urinalysis Under Variable Illumination," *IEEE J. Transl. Eng. Heal. Med.*, vol. 6, pp. 1–11, 2018, doi: 10.1109/JTEHM.2017.2765631.

[13] J. Choi *et al.*, "Soft, skin-integrated multifunctional microfluidic systems for accurate colorimetric analysis of sweat biomarkers and temperature," *ACS Sensors*, vol. 4, no. 2, pp. 379–388, 2019, doi: 10.1021/acssensors.8b01218.

[14] S. J. Kim, D. Kim, and S. Kim, "Simultaneous quantification of multiple biomarkers on a self-calibrating microfluidic paper-based analytic device," *Anal. Chim. Acta*, vol. 1097, pp. 120–126, 2020, doi: 10.1016/j.aca.2019.10.068.

[15] A. M. López-Marzo and A. Merkoçi, “Paper-based sensors and assays: a success of the engineering design and the convergence of knowledge areas,” *Lab Chip*, vol. 16, no. 17, pp. 3150–3176, 2016, doi: 10.1039/C6LC00737F.

[16] A. M. López-Marzo and A. Merkoçi, “Paper-based sensors and assays: a success of the engineering design and the convergence of knowledge areas,” *Lab Chip*, vol. 16, no. 17, pp. 3150–3176, 2016, doi: 10.1039/C6LC00737F.

[17] F. Dincer, Can Bruch, Richard Costa-Rama, Estefanía Fernández-Abedul, Maria Teresa Merkoçi, Arben Manz, Andreas Urban, Gerald Anton Güder, “Disposable Sensors in Diagnostics, Food, and Environmental Monitoring,” *Adv. Mater.*, vol. 31, no. 30, 2019, doi: 10.1002/adma.201806739.

[18] D. Wave, “Quick Reponse (QR) code,” 1994.

[19] K. Yang, H. Peretz-Soroka, Y. Liu, and F. Lin, “Novel developments in mobile sensing based on the integration of microfluidic devices and smartphones,” *Lab Chip*, vol. 16, no. 6, pp. 943–958, 2016, doi: 10.1039/C5LC01524C.

[20] S. M. Russell, A. Doménech-Sánchez, and R. de la Rica, “Augmented Reality for Real-Time Detection and Interpretation of Colorimetric Signals Generated by Paper-Based Biosensors,” *{ACS} Sensors*, vol. 2, no. 6, pp. 848–853, Jun. 2017, doi: 10.1021/acssensors.7b00259.

[21] T. F. Scherr, S. Gupta, D. W. Wright, and F. R. Haselton, “An embedded barcode for ‘connected’ malaria rapid diagnostic tests,” *Lab Chip*, vol. 17, no. 7, pp. 1314–1322, 2017, doi: 10.1039/c6lc01580h.

[22] M. Yuan, Q. Jiang, K.-K. Liu, S. Singamaneni, and S. Chakrabartty, “Towards an Integrated {QR} Code Biosensor: Light-Driven Sample Acquisition and Bacterial Cellulose Paper Substrate,” *{IEEE} Trans. Biomed. Circuits Syst.*, vol. 12, no. 3, pp. 452–460, Jun. 2018, doi: 10.1109/tbcas.2018.2801566.

[23] T. Wang *et al.*, “A novel combination of quick response code and microfluidic paper-based analytical devices for rapid and quantitative detection,” *Biomed. Microdevices*, vol. 20, no. 3, pp. 1–8, 2018, doi: 10.1007/s10544-018-0325-1.

[24] A. Burklund, H. K. Saturley-hall, F. A. Franchina, and J. E. H. J. X. J, “Printable QR code paper microfluidic colorimetric assay for screening volatile biomarkers. ESI,” pp. 1–5.

[25] H. Zhang *et al.*, “Flipped Quick-Response Code Enables Reliable Blood Grouping,” *ACS Nano*, vol. 15, no. 4, pp. 7649–7658, Apr. 2021, doi: 10.1021/acsnano.1c01215.

[26] J. Yang, K. Wang, H. Xu, W. Yan, Q. Jin, and D. Cui, “Talanta Detection platforms for point-of-care testing based on colorimetric , luminescent and magnetic assays : A review,” *Talanta*, vol. 202, no. April, pp. 96–110, 2019, doi: 10.1016/j.talanta.2019.04.054.

[27] M. Ariza-Avidad, A. Salinas-Castillo, M. P. Cuéllar, M. Agudo-Acemel, M. C. Pegalajar, and L. F. Capitán-Vallvey, “Printed Disposable Colorimetric Array for Metal Ion Discrimination,” *Anal. Chem.*, vol. 86, no. 17, pp. 8634–8641, Sep. 2014, doi: 10.1021/ac501670f.

[28] S. Owen, “Zxing Project,” 2014.

[29] C. Callewaert, B. Buysschaert, E. Vossen, V. Fievez, T. Van de Wiele, and N. Boon, “Artificial sweat composition to grow and sustain a mixed human axillary microbiome,” *J. Microbiol. Methods*, vol. 103, pp. 6–8, 2014, doi: 10.1016/j.mimet.2014.05.005.

Figures

Figure 1. Accessory to support the QR code for the colorimetric detection of glucose and lactate. (1) The printed QR code on paper containing the reagents for the determination of glucose and lactate; (2) an absorbent sampling pad; and (3) a transparent screen to assemble the absorbent pad and the QR code.

Figure 2. General scheme of the system.

Figure 3. Architecture of the colorimetric QR code analyser.

Figure 4. a) Saturation of the measured modules of a QR at different colour temperatures before and after both correction methods are applied. Pictures taken with Pocophone F1 device at ISO 400 and 1/125 s exposure time; b) Saturation of measured modules of a QR at different ISOs before and after correction. Pictures taken with automatic white balance and 1/125 s exposure time.

Figure 5. Layered architecture of the developed cloud computing-based system.

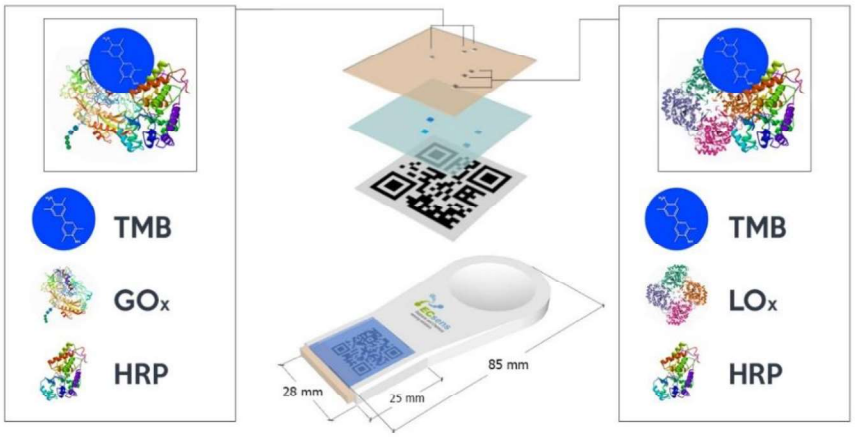

Figure 1

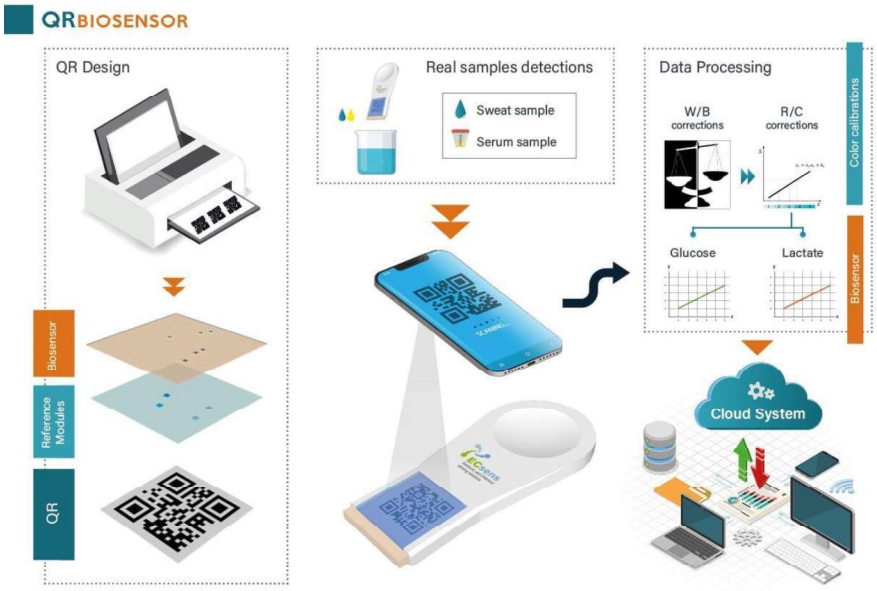

Figure 2

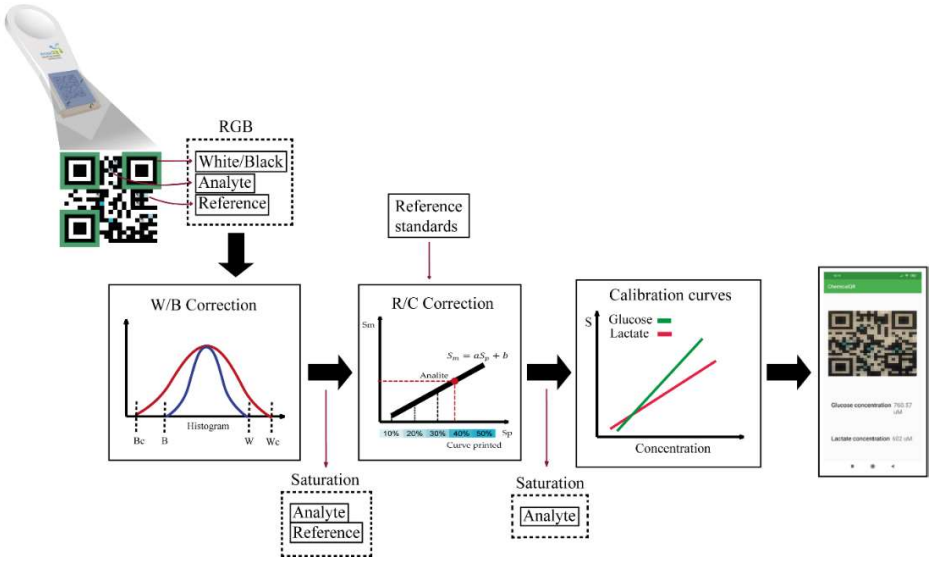

Figure 3

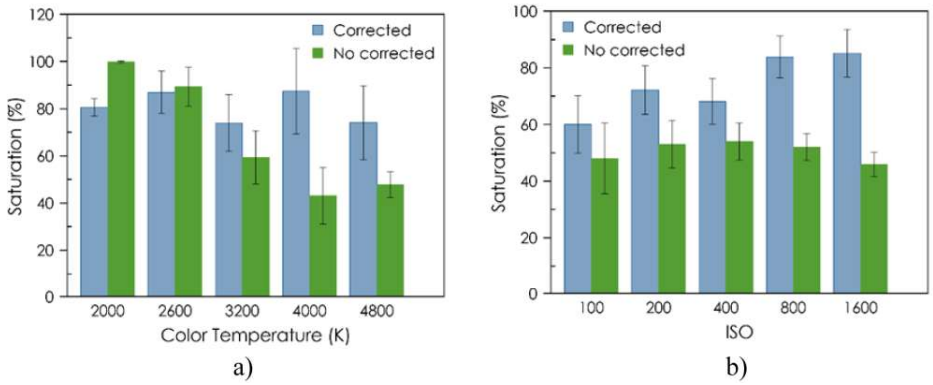

Figure 4

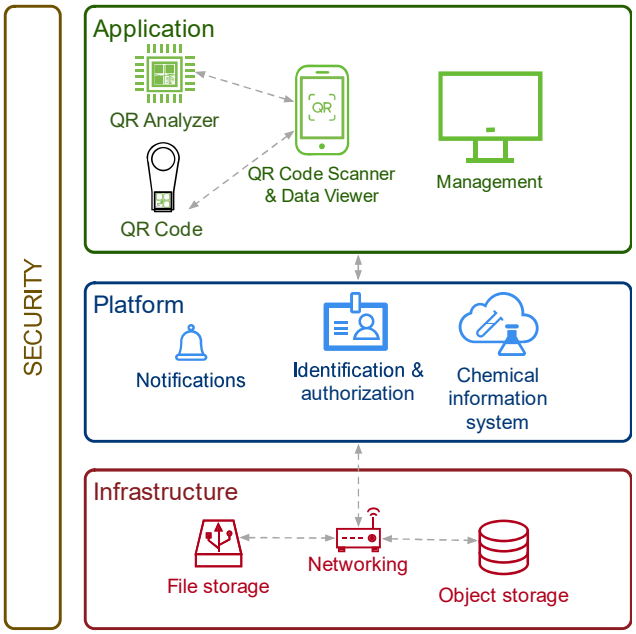

Figure 5

Table 1. Analytical characteristics of QR code for glucose and lactate determination

Analytical parameter	Glucose	Lactate
Measurement range (μM)	197.60 – 1000.00	130.78 – 1000.00
Slope (b)	0.05	0.05

Intercept (a)	15.63	11.37
LOD (µM)	65.21	43.16
LOQ (µM)	197.60	130.78
Precision (%) 200 µM	1.20	0.80
Lifetime (days)	30	30

Table 2. Determination of glucose and lactate in biological samples using a Huawei PSmart device.

Samples	Found	Added	Total found	Recovery %
Glucose (µmol)				
Serum 1	0.00	200	210.2	105.1
Serum 2	0.00	500	516.6	103.3
Serum 3	0.00	800	806.3	100.8
Sweat 1	139.2	200	356.3	105.0
Sweat 2	139.2	500	729.0	114.0
Sweat 3	139.2	800	1037.7	110.5
Lactate (µmol)				
Serum 1	239	200	405.5	92.4
Serum 2	239	500	742.4	100.5
Serum 3	239	800	1075.8	103.6
Sweat 1	135	200	321.0	95.8
Sweat 2	135	500	602.0	94.8
Sweat 3	135	800	859.4	91.9

Table 3. Determination of glucose and lactate in biological samples using a Pocophone F1 device

Samples	Found	Added	Total found	Recovery %
Glucose (µmol)				
Serum 1	0.00	200	235.0	117.5
Serum 2	0.00	500	502.3	100.5
Serum 3	0.00	800	816.3	102.0
Sweat 1	201.3	200	423.7	105.6
Sweat 2	201.3	500	783.2	111.7
Sweat 3	201.3	800	1118.9	111.7
Lactate (µmol)				

Serum 1	219	200	391.0	93.2
Serum 2	219	500	742.4	99.6
Serum 3	219	800	1102.9	108.2
Sweat 1	135	200	321.0	95.8
Sweat 2	135	500	602.0	94.8
Sweat 3	135	800	859.4	91.9